Journal of
Mechanics of
Materials and Structures

ELASTIC ANALYSIS OF CLOSED-FORM SOLUTIONS FOR ADHESIVE
STRESSES IN BONDED SINGLE-STRAP BUTT JOINTS

Gang Li

ELASTIC ANALYSIS OF CLOSED-FORM SOLUTIONS FOR ADHESIVE STRESSES IN BONDED SINGLE-STRAP BUTT JOINTS

GANG LI

In this paper, the adhesive stresses in unbalanced bonded single-strap butt joints are theoretically studied. Mathematical difficulties in the analysis of high order differential equations were solved and closed-form solutions for both the adhesive peel and shear stresses have been successfully developed. In the proposed solutions the adherends and doublers can be different in material and thickness. Peak stresses are located at the bonded overlap edges, especially at the inner edges. In addition, two-dimensional geometrically nonlinear finite element analyses were carried out to study the adhesive stresses in two different bonded butt joints. One was a special butt joint case with the adherends and doubler of identical material and thickness, and the other was a general butt joint case with different adherends and doubler. Good agreement in the adhesive stresses between the closed-form solutions and finite element results has been achieved. The single-strap butt joint actually consists of two single-lap joints; thus, the adhesive stress solutions can be further applied to unbalanced single-lap joints.

1. Introduction

The elastic analysis of bonded joints can be traced back to the 1930s, and was first practiced on balanced single-lap joints by Volkersen [1938]. Since then, extensive theoretical studies have been carried out on this joint configuration [Goland and Reissner 1944; Hart-Smith 1973; Chen and Cheng 1983; Adams and Wake 1984; Oplinger 1994; Tsai and Morton 1994; Li and Lee-Sullivan 2006a; 2006b]. To date, closed-form solutions of balanced single-lap joints for predicting bending moments and shear forces at the overlap edges, as well as the adhesive shear and peel stresses in the adhesive layer, have been well established. A balanced symmetric, adhesive single-lap joint is defined as a single-lap joint made by adhesively bonding two identical adherends. When the two adherends have different geometries and/or mechanical properties, the joints are referred to as unbalanced (see Figure 1(a)). The complexity of this joint configuration is much greater than that of the balanced case. In addition, due to the complicated and tedious derivation and lengthy stress expressions, the corresponding complete closed-form adhesive stress solutions have not been provided in the open literature [Hart-Smith 1973; Williams 1975; Bigwood and Crocombe 1989; Cheng et al. 1991]. With the progress achieved in adhesively bonded single- and double-lap joints (see Figure 1(b)), single-strap butt joint configuration became the subsequent topic of study (see Figure 1(c)). The extent of study on single-strap butt joints was less than that on the single-lap joints and the theoretical progress was slow. This situation could be attributed to the inherent theoretical difficulties in the required mathematics and identification of its potential roles in engineering structural applications, as claimed by Hart-Smith [1985].

Keywords: adhesive stress, closed-form solution, single-strap butt joint, finite element analysis.

(a) Single-lap joint   (b) Double-lap joint
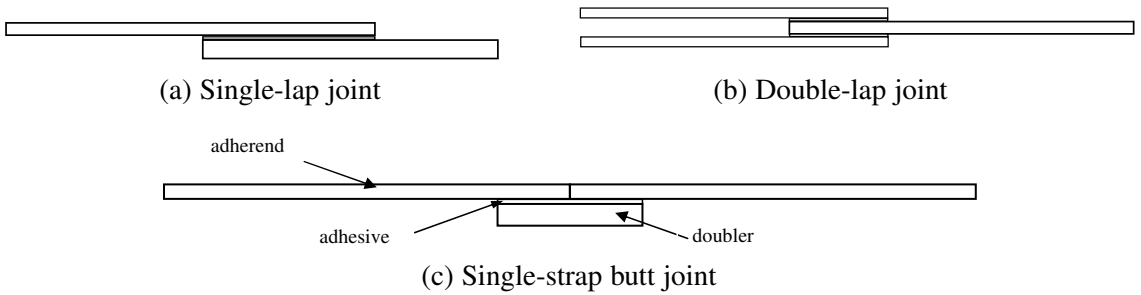
(c) Single-strap butt joint

Figure 1. Several adhesively bonded joint configurations.

A single-strap joint consists of two single-lap joints. For joints with identical doubler and adherends, a special joint case, closed-form adhesive stress solutions can be easily obtained using the same approach as in the balanced single-lap joint configuration. For the butt joints with different doubler and adherends, a coupling relationship exists between the adhesive peel and shear stresses, and the corresponding complete closed-form solutions in explicit expressions in the adhesive stresses have not been reported in the open literature. Delale et al. [1981] reported on a bonded panel-to-substrate joint structure, which could be approximately treated as an unbalanced butt joint configuration with one piece of the adherend bonded with a sort of doubler. They gave general expressions of the closed-form solutions for the adhesive peel and shear stresses, and presented the boundary conditions used to determine the integral constants. Complex terms with nonzero imaginary terms were present in the adhesive stress expressions, the integral constants, and the final expressions of the adhesive stresses, and were not further investigated.

Currently, there is a strong and growing trend towards optimizing the strength, weight, and durability of aircraft structures. The substantial developments in high performance composite structures and special automated fiber placement machines encourage expectations for the extensive application of composite joints to both the secondary and primary structures in aircraft. The fuselage structures for the new generation of aircraft are being built by assembling several precured one-piece composite fuselage barrels. A bonded single-strap butt joint configuration could be one of the possible configurations for the assembly of the fuselage structure. In addition, this joint configuration has a better aerodynamic efficiency than most other joint configurations. As reported by Kweon et al. [2006], the static strength of bonded double-lap joints using film adhesives FM73 could be much higher than that of bolted joints. With the development in joint bonding techniques, the peak peel stress can be effectively reduced, as reported by da Silva and Adams [2007a; 2007b]. To maximize the joint efficiency, an adequate understanding of the variation in adhesive stresses under various influences is essential. This paper presents theoretical explorations of the adhesive stresses in an adhesively bonded general single-strap joint configuration with different adherends and doubler. Without losing generality of the solutions and avoiding unnecessary complexity in the theoretical derivation, the joints will be restricted to being made from isotropic materials. The aim of the work is to obtain closed-form solutions for the adhesive stresses in isotropic butt joints so that the solutions can later be extended to composite joints including unbalanced single-lap joints. The obtained theoretical solutions can be used to quantitatively study the effect of each component on the variation in adhesive stresses, guide practical joint design, and make possible sound bases for practical applications

in the aerospace industry. For the provided complete closed-form solutions, the integration constants are quite long, which should be acceptable for such a complicated analysis of high order differential equations. Furthermore, they can be a solid basis for further effective development of simplified stress solutions for more practical applications in the near future. For the sake of brevity, only the main contents of the adhesive stress derivations are present in this paper. An extended version including a parametric study using the developed closed-form solutions can be found elsewhere [Li 2008].

2. Theoretical formulations

Joint deflection. Secondary bending occurs in butt joints when they are loaded in tension. Within the elastic deformation range, it is appropriate to treat both adherends and doubler as beams using cylindrical bent plate theory, as initially proposed by Goland and Reissner [1944], and then applied by others in works including [Hart-Smith 1973; Cheng et al. 1991; Oplinger 1994; Li and Lee-Sullivan 2006a; Li 2008]. The deformation of a single-strap butt joint in tension is shown in Figure 2. The geometrical nonlinearity induced by the out-of-plane deflection w should be involved in identifying the joint bending
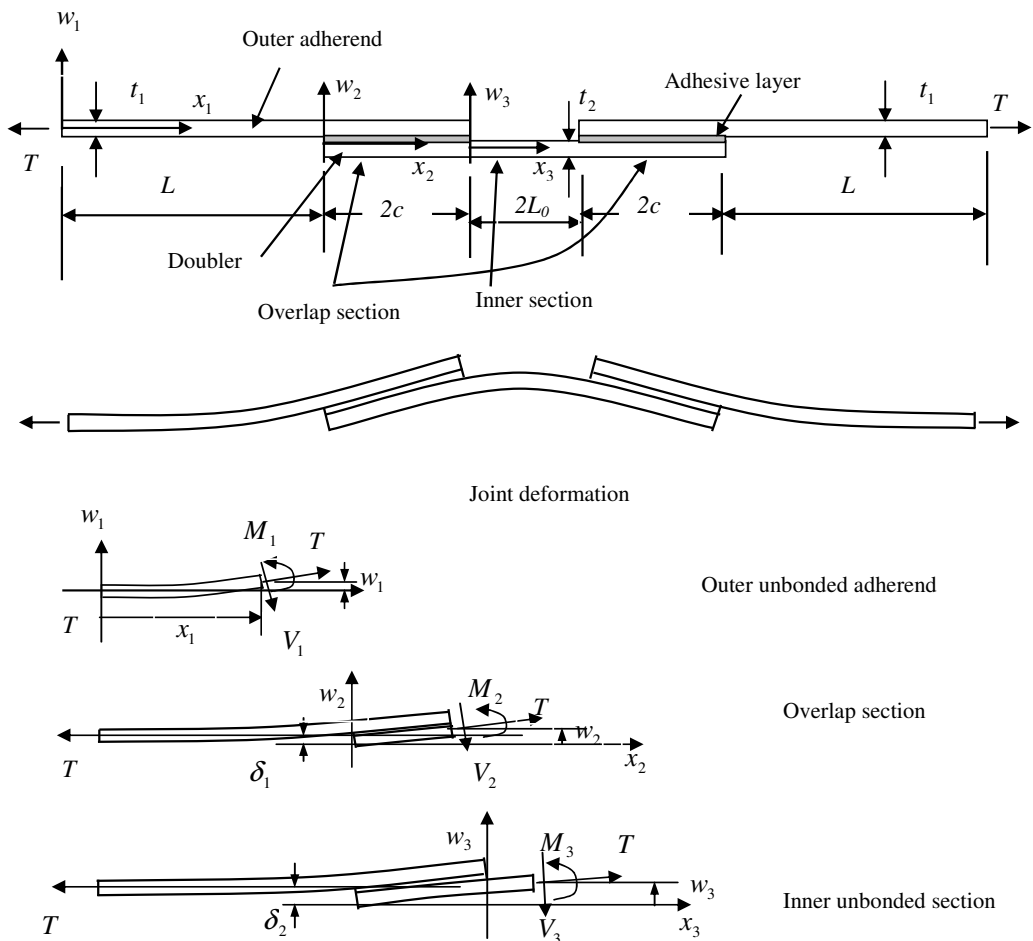

Figure 2. Deformation of the adhesively bonded single-strap butt joint in tension (not to scale).

moment. An accurate joint deflection and shear force can then be determined using cylindrical bent plate or beam theory. The variables in this joint configuration include both dimension and material parameters. The length of the outer unbonded adherend is L, the bonded overlap length is $2c$ on each side, the length of the inner unbonded doubler is $2L_0$, the total length of the doubler is $4c + 2L_0$, and the total joint length is $2L + 4c + 2L_0$. The adherend thickness is t_1 and the doubler thickness is t_2. The plane strain condition is applicable for the joint configuration, and thus, the per-unit-width forces of tensile force, T, the shear force, V_i, and the bending moment, M_i, are the three forces assumed in the joint. By convention, when $i = 1$ the forces are in the outer unbonded adherends, when $i = 2$ the forces are in the bonded overlap section, and when $i = 3$ the forces are in the inner unbonded doubler section. The tensile force T is applicable to any section of the joint.

Brief descriptions of the joint deflection derivation are given in the following. Detailed expressions of the deflection within each section can be found in [Li 2008].

Bending moments and shear forces. The per-unit-width bending moment and shear force at specific positions can be obtained using the relations

$$M_i = D_i \frac{d^2 w_i}{dx_i^2} \quad (i = 1, 2, 3), \qquad V_i = \frac{dM_i}{dx_i} = D_i \frac{d^3 w_i}{dx_i^3} \quad (i = 1, 2, 3), \tag{1a}$$

where

$$D_1 = \frac{E'_{\text{adherend}} t_{\text{adherend}}^3}{12} = \frac{E_1 t_1^3}{12(1 - v_1^2)} \qquad \text{(plane strain)},$$

$$
\begin{aligned}
D_2 &= E'_{\text{adhesive}} \left(\frac{\eta^3}{12} + \eta \left(\delta_1 - \frac{t_{\text{adherend}} + \eta}{2} \right)^2 \right) + E'_{\text{adherend}} \left(\frac{t_{\text{adherend}}^3}{12} + t_{\text{adherend}} \delta_1^2 \right) \\
&\qquad\qquad\qquad\qquad\qquad + E'_{\text{doubler}} \left(\frac{t_{\text{doubler}}^3}{12} + t_{\text{doubler}} (\delta_2 - \delta_1)^2 \right) \\
&\approx E'_{\text{adherend}} \left(\frac{t_{\text{adherend}}^3}{12} + t_{\text{adherend}} \delta_1^2 \right) + E'_{\text{doubler}} \left(\frac{t_{\text{doubler}}^3}{12} + t_{\text{doubler}} (\delta_2 - \delta_1)^2 \right) \\
&= E'_1 \left(\frac{t_1^3}{12} + t_1 \delta_1^2 \right) + E'_2 \left(\frac{t_2^3}{12} + t_2 (\delta_2 - \delta_1)^2 \right),
\end{aligned}
\tag{1b}
$$

$$D_3 = \frac{E'_{\text{doubler}} t_{\text{doubler}}^3}{12} = \frac{E_2 t_2^3}{12(1 - v_2^2)}.$$

The parameter D_i $(i = 1, 2, 3)$ is the per-unit-width bending stiffness in the plane strain condition of the outer unbonded adherends, overlap, and inner unbonded doubler sections, respectively. In the bonded overlap section, the impact of the adhesive stiffness to the stiffness D_2 can be neglected, because it is small enough compared to those of the adherends and doubler. The origins of the coordinate frames are located at the centroid in the left end cross-sectional area of each section. δ_1 and δ_2 are the transverse (vertical) distances between the neutral planes, as shown in Figure 3 and given by

$$\delta_1 = \frac{t_1 + t_2 + 2\eta}{2\left(1 + E'_1 t_1 / (E'_2 t_2)\right)}, \qquad \delta_2 = \frac{t_1 + t_2 + 2\eta}{2}. \tag{1c}$$
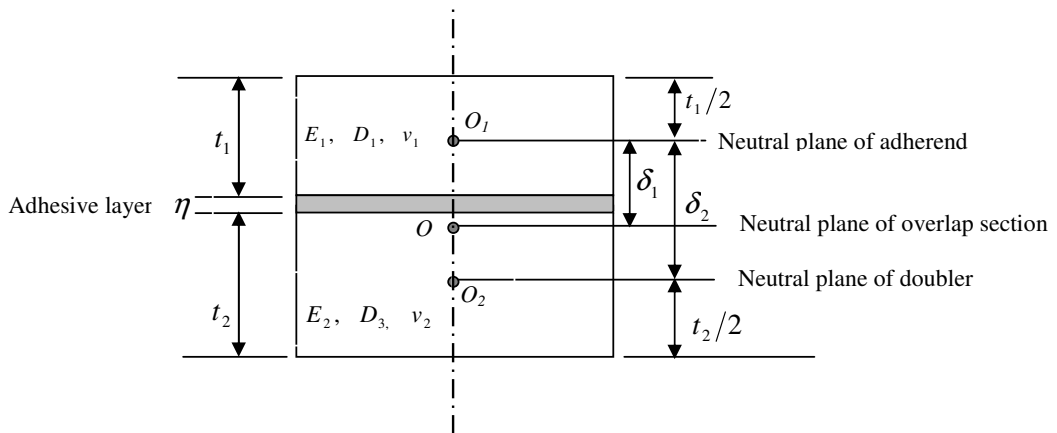
**Figure 3.** Neutral planes of the cross-sectional area of the bonded overlap section.

Overlap section. The sign convention for the positive tensile force, shear force, and bending moment is defined in Figure 4. The subscripts u and d apply to the upper adherend and doubler in the overlap section, respectively.

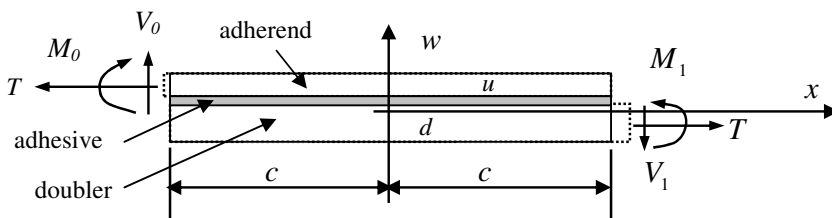The bending moments and shear forces at the two outer overlap edges are

$$M_0 = D_u \frac{d^2 w_1(x_1)}{dx_1^2}\bigg|_{x_1=L}, \qquad V_0 = D_u \frac{d^3 w_1(x_1)}{dx_1^3}\bigg|_{x_1=L}. \tag{2a}$$

The bending moment and shear forces at the two inner overlap edges are

$$M_1 = D_d \frac{d^2 w_3(x_3)}{dx_3^2}\bigg|_{x_3=0}, \qquad V_1 = D_d \frac{d^3 w_3(x_3)}{dx_3^3}\bigg|_{x_3=0}. \tag{2b}$$
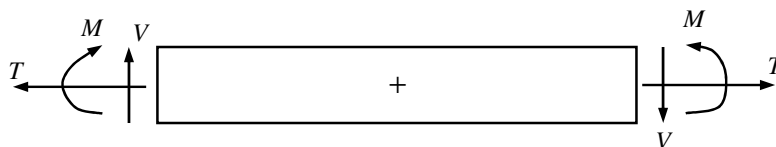
(a) Sign convention (positive force definition)

(b) Coordinate frame in the left overlap section at the overlap centroid and edge forces

Figure 4. Illustrations of force sign convention and the loading condition at the joint overlap edge.
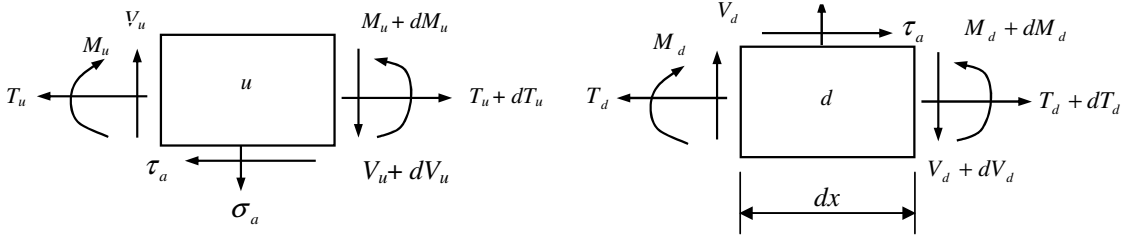
Figure 5. Illustration of loading state in infinitesimal elements for upper adherend (u) and lower doubler (d) in the overlap section.

Please note that the relations, $D_u = D_1$ (the adherend) and $D_d = D_3$ (the doubler) exist throughout the entire paper. To clearly display the variation in moments at the outer and inner overlap edges and directly study the quantitative relationship between the two edge moment magnitudes affected by each joint component and tensile load, these being the edge moments normalized by the moment parameter $(t_1 + \eta)T/2$, the edge moment factors are introduced and defined as

$$k_1 = \frac{2}{(t_1 + \eta)T} M_0 \approx \frac{2M_0}{T t_1} \quad \text{(outer edges)}, \qquad k_2 = \frac{2}{(t_1 + \eta)T} M_1 \approx \frac{2M_1}{T t_1} \quad \text{(inner edges)}. \tag{2c}$$

Adhesive shear and peel stresses. Adhesive stresses can be determined from the equilibrium in the overlap section, as shown in Figure 5, where σ_a is the peel stress, τ_a the shear stress, and η the adhesive thickness. The adherend thickness is t_1 and the doubler thickness is t_2. The force and the moment equilibrium equations for the upper and lower infinitesimal elements in the bonded overlap section can be described by

$$\frac{dM_u}{dx} - V_u - \tau_a\left(\frac{t_1 + \eta}{2}\right) = 0, \qquad \frac{dT_u}{dx} - \tau_a = 0, \qquad \frac{dV_u}{dx} + \sigma_a = 0, \qquad \frac{d^2 w_u}{dx^2} = \frac{M_u}{D_u},$$

$$\frac{dM_d}{dx} - V_d - \tau_a\left(\frac{t_2 + \eta}{2}\right) = 0, \qquad \frac{dT_d}{dx} + \tau_a = 0, \qquad \frac{dV_d}{dx} - \sigma_a = 0, \qquad \frac{d^2 w_d}{dx^2} = \frac{M_d}{D_d}. \tag{3a}$$

The axial strains of the adherend-adhesive and adhesive-doubler interfaces are

$$\varepsilon_{ux} = \frac{du_u}{dx} = \frac{T_u}{E'_u t_1} + \frac{t_1}{2}\frac{M_u}{D_u}, \qquad \varepsilon_{dx} = \frac{du_d}{dx} = \frac{T_d}{E'_d t_2} - \frac{t_2}{2}\frac{M_d}{D_d}, \tag{3b}$$

where $E' = E/(1 - v^2)$ under the plane strain condition.

Generally, the adherends and doubler may behave in a linear elastic manner, but under relatively severe loading and temperature the adhesive may exhibit viscoelastic and/or nonlinear properties. The nonlinearities in the material properties make exact analytical treatment of the structural and material problems very complicated. Therefore, the theoretical analysis was carried out using simplified assumptions. The adherends, doubler, and adhesive were treated as linear elastic materials. For the elastic adhesive layer, the relationships between the adhesive peel and shear stresses and the displacements of the upper adherend and lower doubler can be defined by

$$\frac{\sigma_a}{E_a} = \frac{w_u - w_d}{\eta}, \qquad \frac{\tau_a}{G_a} = \frac{u_u - u_d}{\eta}, \tag{3c}$$

where E_a and G_a are elastic and shear moduli of the adhesive material.

Differentiating Equation (3c) and utilizing these equilibrium relations, the coupling relations existing between the peel and shear stresses can be identified as

$$\frac{d^3\tau_a}{dx^3} + a_1\frac{d\tau_a}{dx} + a_2\sigma_a = 0, \qquad \frac{d^4\sigma_a}{dx^4} + b_1\sigma_a + b_2\frac{d\tau_a}{dx} = 0, \tag{4a}$$

where

$$a_1 = -\frac{G_a}{\eta}\left(\frac{1}{E'_u t_1} + \frac{1}{E'_d t_2} + \frac{t_1(t_1+\eta)}{4D_u} + \frac{t_2(t_2+\eta)}{4D_d}\right), \qquad a_2 = \frac{G_a}{\eta}\left(\frac{t_1}{2D_u} - \frac{t_2}{2D_d}\right),$$

$$b_1 = \frac{E_a}{\eta}\left(\frac{1}{D_u} + \frac{1}{D_d}\right), \qquad\qquad\qquad b_2 = \frac{E_a}{\eta}\left(\frac{t_2+\eta}{2D_d} - \frac{t_1+\eta}{2D_u}\right). \tag{4b}$$

The coupling relations vanish provided the coupling parameters $a_2 = b_2 = 0$, when the same material with identical thickness is used for the adherends and doubler.

3. Solutions for the adhesive stresses

Definition of the butt joints in general and special cases. The general case refers to joints with different adherends and doubler in their materials and/or thicknesses. The special case refers to joints in which the coupling between the adhesive peel and shear stresses vanishes, for instance, in joints with the same material and thickness in the adherends and doubler. For this situation, the adhesive peel and shear stresses can be decoupled as in balanced single-lap joints; thus, it is easy to obtain the closed-form solutions [Oplinger 1994; Li and Lee-Sullivan 2006a; Li 2008].

Efforts to explore the closed-form solutions are carried out for the general butt joint case in the following.

Determination of the adhesive stresses in the general case.

Adhesive shear stress. By eliminating the peel stress in the coupling Equation (4a), the equation of the adhesive shear stress can be written as

$$\frac{d^7\tau_a}{dx^7} + a_1\frac{d^5\tau_a}{dx^5} + b_1\frac{d^3\tau_a}{dx^3} + (a_1b_1 - a_2b_2)\frac{d\tau_a}{dx} = 0. \tag{5a}$$

The characteristic equation of this equation is

$$\lambda^7 + a_1\lambda^5 + b_1\lambda^3 + (a_1b_1 - a_2b_2)\lambda = 0 \tag{5b}$$

(see [AEP 1979; Derrick and Grossman 1987; Kreyszig 1993]). One root is $\lambda_0 = 0$, and then the equation above becomes $\lambda^6 + a_1\lambda^4 + b_1\lambda^2 + (a_1b_1 - a_2b_2) = 0$. Assuming $\phi = \lambda^2$, the equation can be written as $\phi^3 + a_1\phi^2 + b_1\phi + (a_1b_1 - a_2b_2) = 0$. Substituting $\phi = \gamma - a_1/3$ into the above equation [AEP 1979], the above equation becomes

$$\gamma^3 + p\gamma + q = 0, \tag{5c}$$

where

$$p = b_1 - \frac{a_1^2}{3}, \qquad q = \frac{2a_1^3}{27} + \frac{2a_1b_1}{3} - a_2b_2. \tag{5d}$$

We use the classical formula to solve (5c). Setting

$$r' = \sqrt[3]{-\frac{q}{2} + \sqrt{\left(\frac{q}{2}\right)^2 + \left(\frac{p}{3}\right)^3}} \quad \text{and} \quad r'' = \sqrt[3]{-\frac{q}{2} - \sqrt{\left(\frac{q}{2}\right)^2 + \left(\frac{p}{3}\right)^3}},$$

the three roots of (5c) are

$$\gamma_1 = r' + r'', \quad \gamma_2 = \omega r' + \omega^2 r'', \quad \gamma_3 = \omega^2 r' + \omega r'', \tag{5e}$$

where $\omega = (-1 + i\sqrt{3})/2$, $\omega^2 = (-1 - i\sqrt{3})/2$, and $i^2 = -1$. The root γ_1 is real; γ_2 and γ_3, and γ_2^2 and γ_3^2, are complex conjugates and can be further expressed as

$$\gamma_2 = -\frac{\gamma_1}{2} + i\frac{\sqrt{3}}{2}(r' - r''), \quad \gamma_3 = -\frac{\gamma_1}{2} - i\frac{\sqrt{3}}{2}(r' - r''). \tag{5f}$$

Using these expressions, the three roots of parameter ϕ can be expressed as

$$\phi_k = \gamma_k - \frac{a_1}{3} \quad (k = 1, 2, 3). \tag{6a}$$

Thus, the second and third roots of λ for (5b) can be determined as

$$\lambda_{1,2} = \pm\sqrt{\gamma_1 - \frac{a_1}{3}} \quad \left(\text{provided } \gamma_1 - \frac{a_1}{3} \geq 0\right). \tag{6b}$$

The second and third roots of ϕ can be expressed as follows [AEP 1979; Derrick and Grossman 1987; Kreyszig 1993]:

$$\phi_2 = |\phi| \exp(i\beta) = |\phi|(\cos\beta + i\sin\beta), \quad \phi_3 = |\phi| \exp(-i\beta) = |\phi|(\cos\beta - i\sin\beta), \tag{6c}$$

where the argument β is the directed angle from the positive x-axis to the complex vector on the complex plane, given by $\beta = \min\{\beta_1, \beta_2\}$, where the angles are defined within the range from 0 to 2π. The sum of the two angles β_1 and β_2 is 2π.

The modulus, $|\phi|$, of ϕ_2 and ϕ_3 is

$$|\phi| = \sqrt{\left(-\frac{\gamma_1}{2} - \frac{a_1}{3}\right)^2 + \frac{3}{4}(r' - r'')^2}, \tag{6d}$$

The angles are measured in radians and are positive in the counterclockwise sense. For instance, if the angle β_1 is within the range $[0, \pi/2]$, then the angles can be calculated as

$$\beta_1 = \arg\phi_2 = \arctan\frac{(\sqrt{3}/2)(r' - r'')}{-\frac{\gamma_1}{2} - \frac{a_1}{3}} \tag{6e}$$

and $\beta_2 = 2\pi - \beta_1$.

Based on the actual positions of ϕ_2 and ϕ_3 on the complex plane, the angle values can be determined. The real part of ϕ_2 and ϕ_3 is $|\phi|\cos\beta = -\gamma_1/2 - a_1/3$, and the imaginary parts of the ϕ_2 and ϕ_3 are

$$\pm|\phi|\sin\beta = \pm\frac{\sqrt{3}}{2}(r' - r'').$$

Based on (6c), the remaining four roots of λ can then be determined as

$$|\phi|^{\frac{1}{2}}\left(\cos\frac{\beta}{2}+i\,\sin\frac{\beta}{2}\right),\ -|\phi|^{\frac{1}{2}}\left(\cos\frac{\beta}{2}+i\,\sin\frac{\beta}{2}\right),\ |\phi|^{\frac{1}{2}}\left(\cos\frac{\beta}{2}-i\,\sin\frac{\beta}{2}\right),\ -|\phi|^{\frac{1}{2}}\left(\cos\frac{\beta}{2}-i\,\sin\frac{\beta}{2}\right). \quad (6f)$$

Expression of the adhesive shear stress. Provided $\phi_1 = \gamma_1 - a_1/3 \geq 0$, the general solution of the adhesive shear stress can be expressed as

$$\tau_a = C_0 + C_1 \cosh\left(x\sqrt{\gamma_1 - \frac{a_1}{3}}\right) + C_2 \sinh\left(x\sqrt{\gamma_1 - \frac{a_1}{3}}\right)$$
$$+ C_3 \cosh\left(x\,|\phi|^{\frac{1}{2}}\cos\frac{\beta}{2}\right)\cos\left(x\,|\phi|^{\frac{1}{2}}\sin\frac{\beta}{2}\right) + C_4 \sinh\left(x\,|\phi|^{\frac{1}{2}}\cos\frac{\beta}{2}\right)\cos\left(x\,|\phi|^{\frac{1}{2}}\sin\frac{\beta}{2}\right)$$
$$+ C_5 \cosh\left(x\,|\phi|^{\frac{1}{2}}\cos\frac{\beta}{2}\right)\sin\left(x\,|\phi|^{\frac{1}{2}}\sin\frac{\beta}{2}\right) + C_6 \sinh\left(x\,|\phi|^{\frac{1}{2}}\cos\frac{\beta}{2}\right)\sin\left(x\,|\phi|^{\frac{1}{2}}\sin\frac{\beta}{2}\right). \quad (7a)$$

In this expression, all seven terms are real (no imaginary part). This shear stress can be directly used for practical joint analysis under the influence of joint components and external loading conditions. This shear stress expression is more practical than the one given in [Delale et al. 1981], where imaginary and real terms were used together.

The seven constants C_j (where j ranges from 0 to 6) can be determined using the following seven boundary conditions:

$$\int_{-c}^{c} \tau_a\,dx = -T.$$

$$\left.\frac{d\tau_a}{dx}\right|_{x=-c} = \left.\frac{G_a}{\eta}\frac{d}{dx}(u_u - u_d)\right|_{x=-c} = \left.\frac{G_a}{\eta}\left(\frac{T}{E'_u t_1} + \frac{t_1}{2}\frac{M_u}{D_u}\right)\right|_{x=-c} = \frac{G_a}{\eta}\left(\frac{T}{E'_u t_1} + \frac{t_1}{2}\frac{M_0}{D_u}\right),$$

$$\left.\frac{d\tau_a}{dx}\right|_{x=c} = \left.\frac{G_a}{\eta}\frac{d}{dx}(u_u - u_d)\right|_{x=c} = \frac{G_a}{\eta}\left(-\frac{T}{E'_u t_2} + \frac{t_2}{2}\frac{M_d}{D_d}\right)\Bigg|_{x=c} = \frac{G_a}{\eta}\left(-\frac{T}{E'_d t_2} + \frac{t_2}{2}\frac{M_1}{D_d}\right),$$

$$\left.\frac{d^2\tau_a}{dx^2} + a_1\tau_a\right|_{x=-c} = \left.\frac{G_a}{\eta}\frac{t_1 V_u}{2 D_u}\right|_{x=-c} = \frac{G_a}{\eta}\frac{t_1}{2}\frac{V_0}{D_u}, \quad (7b)$$

$$\left.\frac{d^2\tau_a}{dx^2} + a_1\tau_a\right|_{x=c} = \left.\frac{G_a}{\eta}\frac{t_2 V_d}{2 D_d}\right|_{x=c} = \frac{G_a}{\eta}\frac{t_2}{2}\frac{V_1}{D_d},$$

$$\left.\frac{d^5\tau_a}{dx^5} + a_1\frac{d^3\tau_a}{dx^3}\right|_{x=-c} = \left.-a_2\frac{E_a}{\eta}\frac{M_u}{D_u}\right|_{x=-c} = -a_2\frac{E_a}{\eta}\frac{M_0}{D_u},$$

$$\left.\frac{d^5\tau_a}{dx^5} + a_1\frac{d^3\tau_a}{dx^3}\right|_{x=c} = \left.a_2\frac{E_a}{\eta}\frac{M_d}{D_d}\right|_{x=c} = a_2\frac{E_a}{\eta}\frac{M_1}{D_d},$$

The expressions of the seven constants in the adhesive shear stress are given in the Online Supplement. The above first boundary condition is obtained through the equilibrium relation of the joint adherend tensile load with the integral of the resulting shear stress in the adhesive layer. The rest of the six boundary conditions relate different derivatives of the adhesive shear stress at the outer and inner overlap ends with the applied loads at the same positions. Assuming continuity of axial strains in the adherends

and doubler at the interfaces with the adhesive layer and the adhesive stresses in the adhesive layer, the second and third boundary conditions at the two overlap ends are obtained by combining the first derivative of the adhesive shear stress in (3c) and the expressions of the axial strains at the adherend-adhesive and adhesive-doubler interfaces in (3b). The adhesive shear stress in (3c) is differentiated twice, using the equilibrium equations of moment and tensile force in (3a) to substitute for the fourth and fifth boundary conditions. To obtain the sixth and seventh boundary conditions for the uncoupled adhesive shear stress, two differentiations are applied to the first coupled adhesive stress equation in (4a) with the aid of the peel stress expression in (3c) and moment-curvature relation in (1a).

Adhesive peel stress. Exploration of the closed-form solution for the adhesive peel stress should be carried out based on its fundamental behavior expressed in (4a). This nonhomogeneous equation degrades to its corresponding homogeneous equation in the special butt joint case when the coupling parameter b_2 vanishes. The nonhomogeneous equation can be investigated using variation of constants or Lagrange's method [AEP 1979; Derrick and Grossman 1987]. The general solution is established by combining the general solution of the homogeneous equation and any one particular solution of the nonhomogeneous equation. If we define

$$X = x \sqrt[4]{\frac{b_1}{4}},$$

the general solution of the homogeneous equation is

$$\sigma_{aH} = C_{1H} \cosh X \cos X + C_{2H} \sinh X \cos X + C_{3H} \cosh X \sin X + C_{4H} \sinh X \sin X. \quad (8a)$$

One particular solution for the nonhomogeneous equation can be expressed in the form

$$\sigma_{ap} = G_{1p}(x) \cosh X \cos X + G_{2p}(x) \sinh X \cos X + G_{3p}(x) \cosh X \sin X + G_{4p}(x) \sinh X \sin X, \quad (8b)$$

where the functions $G_{1p}(x)$, $G_{2p}(x)$, $G_{3p}(x)$, and $G_{4p}(x)$ are determined using the following simultaneous equations [AEP 1979; Derrick and Grossman 1987]:

$$G'_{1p}(x) \cosh X \cos X + G'_{2p}(x) \sinh X \cos X + G'_{3p}(x) \cosh X \sin X + G'_{4p}(x) \sinh X \sin X = 0,$$

$$G'_{1p}(x) \frac{d}{dx}(\cosh X \cos X) + G'_{2p}(x) \frac{d}{dx}(\sinh X \cos X)$$
$$+ G'_{3p}(x) \frac{d}{dx}(\cosh X \sin X) + G'_{4p}(x) \frac{d}{dx}(\sinh X \sin X) = 0,$$

$$G'_{1p}(x) \frac{d^2}{dx^2}(\cosh X \cos X) + G'_{2p}(x) \frac{d^2}{dx^2}(\sinh X \cos X) \quad (8c)$$
$$+ G'_{3p}(x) \frac{d^2}{dx^2}(\cosh X \sin X) + G'_{4p}(x) \frac{d^2}{dx^2}(\sinh X \sin X) = 0,$$

$$G'_{1p}(x) \frac{d^3}{dx^3}(\cosh X \cos X) + G'_{2p}(x) \frac{d^3}{dx^3}(\sinh X \cos X)$$
$$+ G'_{3p}(x) \frac{d^3}{dx^3}(\cosh X \sin X) + G'_{4p}(x) \frac{d^3}{dx^3}(\sinh X \sin X) = -b_2 \frac{d\tau_a}{dx}.$$

The expressions for $G_{ip}(x)$ $(i = 1, \ldots, 4)$ functions are given in the Online Supplement. The general solution for the adhesive peel stress in the general butt joint case can be established as

$$\sigma_a = \sigma_{aH} + \sigma_{ap}$$

$$= C_{1H} \cosh X \cos X + C_{2H} \sinh X \cos X + C_{3H} \cosh X \sin X + C_{4H} \sinh X \sin X$$

$$+ G_{1p}(x) \cosh X \cos X + G_{2p}(x) \sinh X \cos X + G_{3p}(x) \cosh X \sin X + G_{4p}(x) \sinh X \sin X. \quad (8d)$$

The expressions for the constants C_{1H}, C_{2H}, C_{3H}, and C_{4H} are also given in the Online Supplement, and are determined using the boundary conditions

$$\left. \frac{d^2\sigma_a}{dx^2} \right|_{x=-c} = \frac{E_a}{\eta} \frac{M_u}{D_u} \bigg|_{x=-c} = \frac{E_a}{\eta} \frac{M_0}{D_u}, \qquad \left. \frac{d^2\sigma_a}{dx^2} \right|_{x=c} = -\frac{E_a}{\eta} \frac{M_d}{D_d} \bigg|_{x=c} = -\frac{E_a}{\eta} \frac{M_1}{D_d},$$

$$\left. \frac{d^3\sigma_a}{dx^3} + b_2\tau_a \right|_{x=-c} = \frac{E_a}{\eta} \frac{V_u}{D_u} \bigg|_{x=-c} = \frac{E_a}{\eta} \frac{V_0}{D_u}, \qquad \left. \frac{d^3\sigma_a}{dx^3} + b_2\tau_a \right|_{x=c} = -\frac{E_a}{\eta} \frac{V_d}{D_d} \bigg|_{x=c} = -\frac{E_a}{\eta} \frac{V_1}{D_d}. \quad (8e)$$

These four boundary conditions relate the derivatives of the adhesive peel stress with the applied loads at the outer and inner overlap ends. Two differentiations are conducted on the peel stress expression in (3c) with the aid of the moment-curvature relation in (1a) to obtain the first two boundary conditions. One more differentiation is applied to the second derivative of the peel stress expression with the aid of the moment equilibrium relation in (3a) to obtain the third and fourth boundary conditions.

Joint special case: parameters of $a_2 = b_2 = 0$. It can be seen from (4b) that the coupling parameters a_2 and b_2 vanish when the butt joints are balanced, a special case. The adhesive shear and peel stresses are then decoupled. The other two parameters in (4b) are

$$a_1 = -\frac{G_a}{\eta} \left(\frac{2}{E't} + \frac{t(t+\eta)}{2D} \right), \qquad b_1 = \frac{2E_a}{\eta D}. \quad (9a)$$

The shear and peel stress equations can be simplified as

$$\frac{d^3\tau_a}{dx^3} + a_1 \frac{d\tau_a}{dx} = 0, \qquad \frac{d^4\sigma_a}{dx^4} + b_1\sigma_a = 0. \quad (9b)$$

Adhesive shear stress. The general solution for the adhesive shear stress is then

$$\tau_a = C_{0S} + C_{1S} \cosh \left(x\sqrt{\frac{G_a}{\eta} \left(\frac{2}{E't} + \frac{t(t+\eta)}{2D} \right)} \right) + C_{2S} \sinh \left(x\sqrt{\frac{G_a}{\eta} \left(\frac{2}{E't} + \frac{t(t+\eta)}{2D} \right)} \right). \quad (10)$$

The expressions of these three constants, C_{iS} $(i = 0, 1, 2)$, are given in the Online Supplement and are determined using the three boundary conditions

$$\int_{-c}^{c} \tau_a\, dx = -T, \qquad \left. \frac{d\tau_a}{dx} \right|_{x=-c} = \frac{G_a}{\eta} \left(\frac{T}{E'_u t_1} + \frac{t_1}{2} \frac{M_u}{D_u} \right) \bigg|_{x=-c}, \qquad \left. \frac{d\tau_a}{dx} \right|_{x=c} = \frac{G_a}{\eta} \left(-\frac{T}{E'_d t_2} + \frac{t_2}{2} \frac{M_d}{D_d} \right) \bigg|_{x=c}.$$

Similarly to the general butt joint case, the first boundary condition is the equilibrium relation in the adherend between the applied tensile load with the integral of the resulting shear stress in the adhesive layer. The second and third boundary conditions relate the first derivative of shear stress to the loads at

the two overlap ends, and are obtained by combining the first derivative of the adhesive shear stress in (3c) with the expressions of the axial strains at the adherend-adhesive and adhesive-doubler interfaces in (3b).

Adhesive peel stress. The general solution for the adhesive peel stress is

$$\sigma_a = C_{3S} \cosh X \cos X + C_{4S} \sinh X \cos X + C_{5S} \cosh X \sin X + C_{6S} \sinh X \sin X. \tag{11}$$

The constants C_{iS} $(i = 3, 4, 5, 6)$ are given in the Online Supplement. They are determined using the boundary conditions

$$\frac{d^2\sigma_a}{dx^2}\Big|_{x=-c} = \frac{E_a}{\eta} \frac{M_u}{D_u}\Big|_{x=-c} = \frac{E_a}{\eta} \frac{M_0}{D}, \qquad \frac{d^2\sigma_a}{dx^2}\Big|_{x=c} = -\frac{E_a}{\eta} \frac{M_d}{D_d}\Big|_{x=c} = -\frac{E_a}{\eta} \frac{M_1}{D},$$

$$\frac{d^3\sigma_a}{dx^3}\Big|_{x=-c} = \frac{E_a}{\eta} \frac{V_u}{D_u}\Big|_{x=-c} = \frac{E_a}{\eta} \frac{V_0}{D}, \qquad \frac{d^3\sigma_a}{dx^3}\Big|_{x=c} = -\frac{E_a}{\eta} \frac{V_d}{D_d}\Big|_{x=c} = -\frac{E_a}{\eta} \frac{V_1}{D}.$$

As in the general butt joint case, the above four boundary conditions relate the derivatives of the adhesive peel stress with the applied loads at the outer and inner overlap ends of the balanced butt joint.

Consistence of the adhesive stresses from the general to the special joint cases. The derivations in the closed-form stress solutions were carried out based on their fundamental equations, thus, when the general case approaches the special butt joint case, both the adhesive peel and shear stresses will converge to their corresponding adhesive stresses in the special joint case, which has been validated in [Li 2008].

Validation of the closed-form solutions of the adhesive stresses using finite element methods. Due to the geometrical nonlinearity caused by the secondary bending deformation in butt joints, two-dimensional geometrically nonlinear finite element (FE) analyses were carried out under the plane strain condition, using MSC Patran and Marc version 2008r1. Linear elastic material properties were used for the FE analyses. Two different joint situations, as given in Table 1 and Figure 6, were considered. The FE results obtained for the adhesive stresses were compared with the corresponding closed-form solutions.

Assuming a small clearance in the joint, a gap of 0.02 mm was assumed to represent the inner section length without adherends and adhesive, as shown in Figure 6. Two elements were used through the adhesive thickness. A fine mesh was applied to the overlap edge areas. Ten elements were used across

Item	Mechanical parameters	Length (mm)	Thickness (mm)
Adherends	$E = 70\,\text{GPa}$, $v = 0.3$	$L = 50$ (each outer adherend)	$t_1 = 2.1$
Doubler	$E = 70\,\text{GPa}$, $v = 0.3$	$4c + 2L_0 = 101.6$ (inner section length of $2L_0 = 0.02$)	$t_2 = 2.1$ and 3.2 for special and general (thicker doubler) cases
Adhesive	$E_a = 3\,\text{GPa}$, $v_a = 0.3$	$4c = 101.58$	$\eta = 0.15$

Table 1. Parameters for the unit width single-strap butt joint. The total gauge length of the joint is $2L + 4c + 2L_0 = 201.6$ mm.
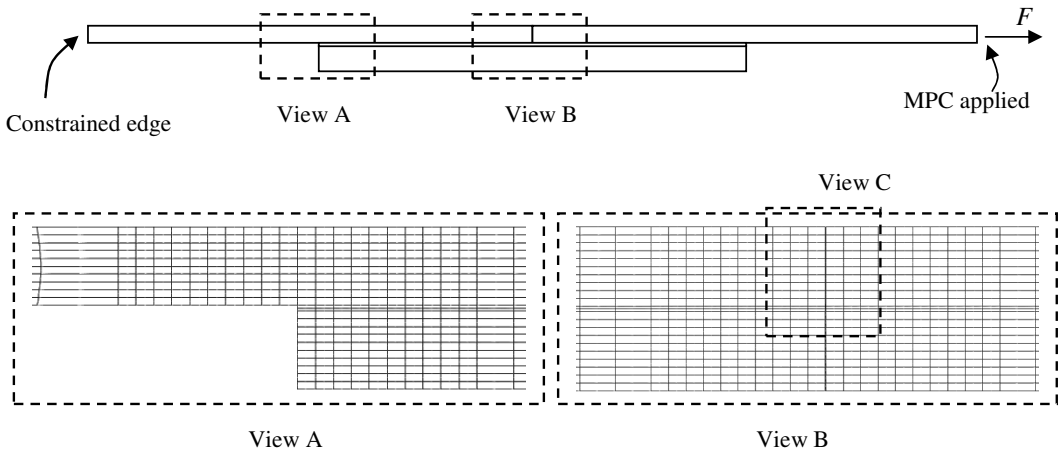
(a) Special case, 2.1 mm thick doubler and adherends
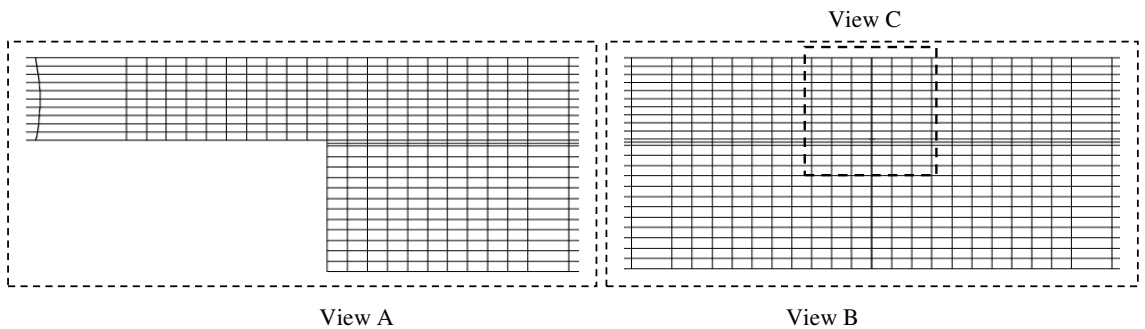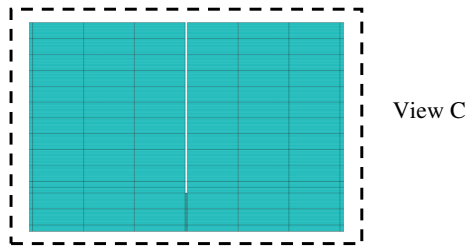
(b) Generai case, 3.2 mm thick doubler and 2.1 thick mm adherends

Figure 6. Schematic diagrams for the two simulated butt joints with a 0.02 mm inner gap section for both adherends and adhesive for the special (2.1 mm doubler) and general (3.2 mm doubler) joints.

the adherends and doubler thicknesses for the special case, and 12 elements were used for the 3.2 mm thick doubler. A total of 3,284 eight-node quadrilateral elements with 10,273 nodes were created for the special case. A total of 3,516 eight-node quadrilateral elements with 10,971 nodes were generated for the thicker doubler general case joint. The left edge was clamped without any displacement in both the horizontal and vertical directions, while the right adherend far end edge was uniformly loaded with a
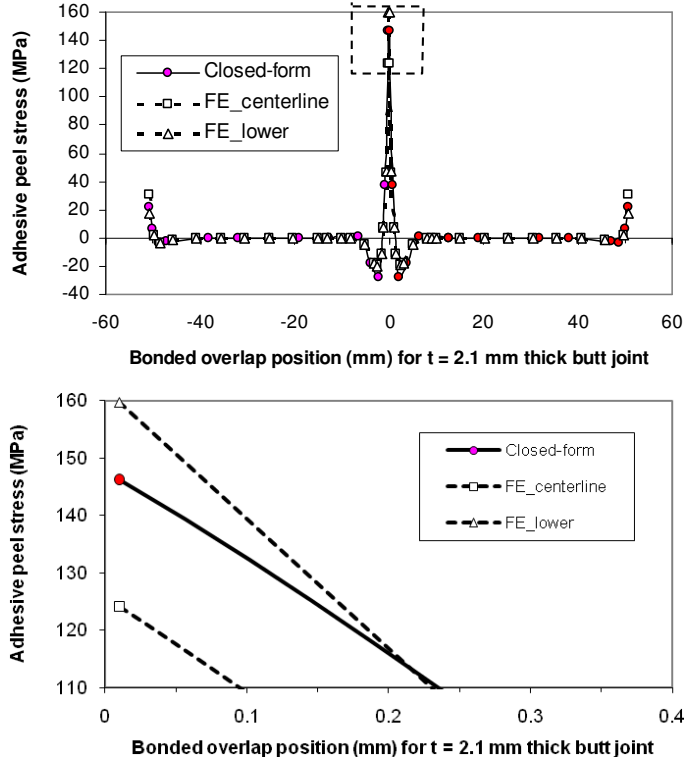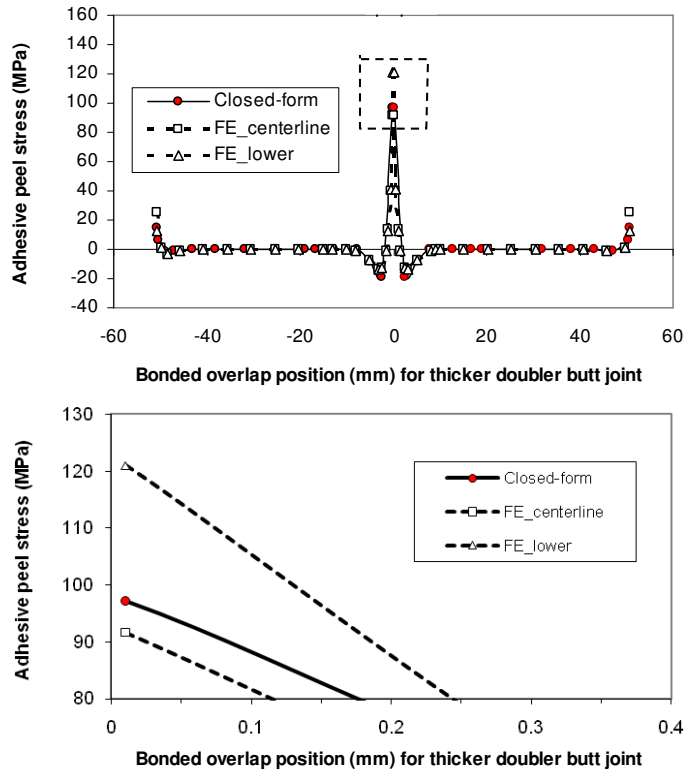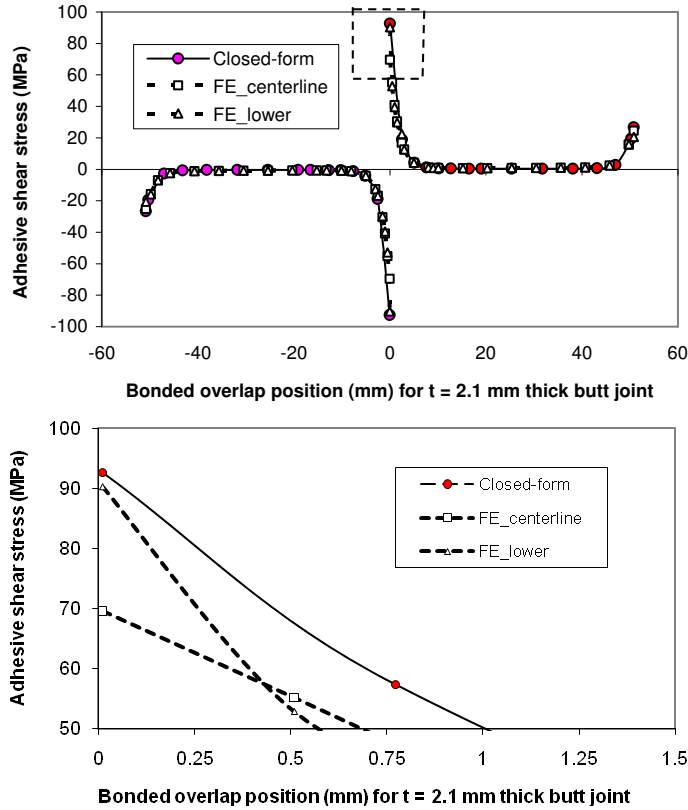
Figure 7. Comparison of the adhesive peel stresses obtained from closed-form solutions and FE results for a special butt joint with identical adherends and doubler (above) with dashed box marking the detail (below). FE_lower refers to the lower path along the midnodes of the lower adhesive layer elements.

tensile stress of 100 MPa. Multipoint-constrain conditions were applied to the right edge nodes having the same displacement during the tensile loading stage.

Comparison of the adhesive stresses between the closed-form solutions and FE results. Five nodes were used through the thickness of the adhesive layer. The peel and shear stresses at the nodes along the adherend-adhesive or adhesive-doubler interface are dominated by the mechanical parameters of both the adherend (or doubler) and adhesive, and cannot be treated as the adhesive stresses. Thus, the adhesive stresses at the upper element midnode, adhesive centerline, and lower elements midnode were extracted and analyzed. The stresses at the lower node were greater than the corresponding stresses at the centerline and upper node. The average stresses along the three paths were identical to the stresses along the centerline. For the closed-form stress solutions, the first step was to determine the bonded overlap edge forces such as the bending moments and shear forces as introduced in Section 2 and elsewhere [Li 2008], then to follow the steps in Section 3, as well as the Online Supplement, to get the adhesive stresses. Variations in the adhesive peel and shear stresses obtained from the closed-form solutions and finite element results are presented in Figures 7–10 for both butt joint cases. Based on these figures, the following observations can be made: the adhesive stresses are uniform in the thickness direction except at the overlap edge nodes; high stresses are present in the vicinity of the overlap edges, the highest
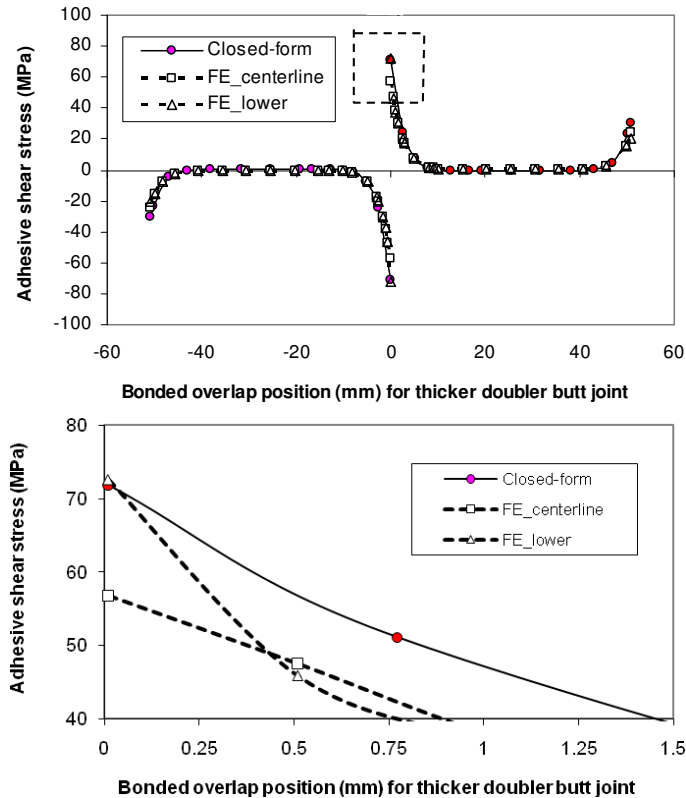
Figure 8. Comparison of the adhesive peel stresses obtained from closed-form solutions and FE results for a general butt joint with 2.1 mm thick adherends and a 3.2 mm thick doubler. FE_lower refers to the lower path along the midnodes of the lower adhesive layer elements.

being at the inner overlap edge position; the stress magnitudes are lower using the thicker doubler; the closed-form solutions are approximately the same as the FE results, except at the edge positions; and at the inner overlap edge position, the peel stresses obtained from the closed-form solutions are within the FE stresses at the centerline and lower path nodes, and the shear stresses obtained from the closed-form solutions are almost identical to the FE results at the lower path nodes and slightly larger than the centerline values. The peak stress values and stress singularity, which existed at the adherend-adhesive and adhesive-doubler interfaces in the vicinity of the overlap edges, are not within the scope of the paper, and thus were not covered in the current FE analyses.

The above comparisons clearly show that the closed-form stress solutions are reliable and accurate in predicting the stress variations. The closed-form stress solutions can also be used to analyze the mode I and mode II strain energy release rates for cohesive crack propagation behavior in a generic situation of butt joints using the approach suggested by Hu [1995] on the single-lap joints.

Figure 9. Comparison of the adhesive shear stresses obtained from closed-form solutions and FE results for a special butt joint with identical adherends and doubler.

4. Concluding remarks

In the study of unbalanced butt joint, the derived high order differential equation was the same as the one initially obtained by Delale et al. [1981] for the uncoupled adhesive shear stress. They provided general stress expressions containing complex terms with nonzero imaginary terms, and did not present the final complete adhesive stress solutions. Among the seven boundary conditions, two were slightly different. However, the impact on the final solutions could be neglected based on our previous study [Li and Lee-Sullivan 2006a]. Due to the page limit, the study of the impact of small differences on the set of boundary conditions on the adhesive stress variation is not carried further. Difficulties and complexities in the derivation process using these high order differential equations have been solved. Closed-form solutions for the adhesive peel and shear stresses have been successfully developed in this paper for the general butt joint case. Good agreement was achieved in the adhesive stresses obtained from the closed-form solutions and finite element results for both the special and general butt joints. The obtained results validate that the used boundary conditions are accurate. Since the closed-form solutions have been obtained from their fundamental behavior equations, the consistence of the adhesive stresses between the general and special joint cases can be theoretically ensured. Moreover, the obtained stress solutions allows the quantitatively study of the effect of each joint component on the variation in the

Figure 10. Adhesive shear stresses obtained from closed-form solutions and FE results for a general butt joint with 2.1 mm thick adherends and a 3.2 mm thick doubler.

adhesive stresses for more joint geometries and materials, as can be found elsewhere [Li 2008]. Thus, a practical evaluation of this joint configuration can be easily carried out using the Excel spreadsheet tool. Usually the length of the inner gap section (the inner unbonded doubler section) in a butt joint is very small and much shorter than the outer adherend length; the two single-lap joints of the butt joint should be then treated as in the unbalanced single-lap joint case. Thus, the adhesive stress solutions obtained from the butt joint configuration can be applied to the unbalanced single-lap joint case if the overlap edge loads are known. The next stage could be: the exploration of the simplified stress solutions for better practical applications, the development of the adhesive stresses in composite butt joints, and the identification of the proper hole positions for introducing extra fasteners to fabricate a strong hybrid attached joint.

References

[Adams and Wake 1984] R. D. Adams and W. C. Wake, *Structural adhesive joints in engineering*, Elsevier, London, 1984.

[AEP 1979] Editorial group, *Mathematics handbook*, Advanced Education Press (AEP), Beijing, 1979. In Chinese.

[Bigwood and Crocombe 1989] D. A. Bigwood and A. D. Crocombe, "Elastic analysis and engineering design formulae for bonded joints", *Int. J. Adhes. Adhes.* **9**:4 (1989), 229–242.

[Chen and Cheng 1983] D. Chen and S. Cheng, "An analysis of adhesive-bonded single-lap joints", *J. Appl. Mech.* (*ASME*) **50**:1 (1983), 109–115.

[Cheng et al. 1991] S. Cheng, D. Chen, and Y. Shi, "Analysis of adhesive-bonded joints with nonidentical adherends", *J. Eng. Mech.* (*ASCE*) **117**:3 (1991), 605–623.

[Delale et al. 1981] F. Delale, F. Erdogan, and M. N. Aydinoglu, "Stresses in adhesively bonded joints: a closed-form solution", *J. Compos. Mater.* **15**:3 (1981), 249–271.

[Derrick and Grossman 1987] W. R. Derrick and S. I. Grossman, *A first course in differential equations with applications*, 3rd ed., West Publishing Company, St. Paul, MN, 1987.

[Goland and Reissner 1944] M. Goland and E. Reissner, "The stresses in cemented joints", *J. Appl. Mech.* (*ASME*) **11** (1944), A17–A27.

[Hart-Smith 1973] L. J. Hart-Smith, "Adhesive-bonded single-lap joints", Contractor Report 112236, NASA Langley Research Center, Hampton, VA, 1973, Available at http://tinyurl.com/NASA-CR-112236.

[Hart-Smith 1985] L. J. Hart-Smith, "Designing to minimize peel stresses in adhesive-bonded joints", pp. 238–266 in *Delamination and debonding of materials* (Pittsburgh, PA, 1983), edited by W. S. Johnson, ASTM Special Technical Publication **876**, American Society for Testing and Materials, Philadelphia, 1985.

[Hu 1995] G. Hu, "Mixed mode fracture analysis of adhesive lap joints", *Compos. Eng.* **5**:8 (1995), 1043–1050.

[Kreyszig 1993] E. Kreyszig, *Advanced engineering mathematics*, 7th ed., Wiley, New York, 1993.

[Kweon et al. 2006] J.-H. Kweon, J.-W. Jung, T.-H. Kim, J.-H. Choi, and D.-H. Kim, "Failure of carbon composite-to-aluminum joints with combined mechanical fastening and adhesive bonding", *Compos. Struct.* **75**:1–4 (2006), 192–198.

[Li 2008] G. Li, "Exploration of closed-form solutions for adhesive stresses in adhesively bonded single-strap butt joints", Technical report LTR-SMPL-2008-0174, National Research Council Canada, Institute for Aerospace Research, Ottawa, ON, 2008.

[Li and Lee-Sullivan 2006a] G. Li and P. Lee-Sullivan, "Re-visiting the beam models for adhesively bonded single-lap joints, I: Comparison of bending moment predictions", *Can. Aeronaut. Space. J.* **52**:4 (2006), 149–171.

[Li and Lee-Sullivan 2006b] G. Li and P. Lee-Sullivan, "Re-visiting the beam models for adhesively bonded single-lap joints, II: Comparison of adhesive stress predictions", *Can. Aeronaut. Space. J.* **52**:4 (2006), 173–180.

[Oplinger 1994] D. W. Oplinger, "Effects of adherend deflections in single lap joints", *Int. J. Solids Struct.* **31**:18 (1994), 2565–2587.

[da Silva and Adams 2007a] L. F. M. da Silva and R. D. Adams, "Adhesive joints at high and low temperatures using similar and dissimilar adherends and dual adhesives", *Int. J. Adhes. Adhes.* **27**:3 (2007), 216–226.

[da Silva and Adams 2007b] L. F. M. da Silva and R. D. Adams, "Techniques to reduce the peel stresses in adhesive joints with composites", *Int. J. Adhes. Adhes.* **27**:3 (2007), 227–235.

[Tsai and Morton 1994] M. Y. Tsai and J. Morton, "An evaluation of analytical and numerical solutions to the single-lap joint", *Int. J. Solids Struct.* **31**:18 (1994), 2537–2563.

[Volkersen 1938] O. Volkersen, "Die Nietkraftverteilung in zugbeanspruchten Nietverbindungen mit konstanten Laschenquerschnitten", *Luftfahrtforsch.* **15** (1938), 41–47.

[Williams 1975] J. H. Williams, Jr., "Stress in adhesive between dissimilar adherends", *J. Adhesion* **7**:2 (1975), 97–107.

GANG LI: Gang.Li@nrc-cnrc.gc.ca
Structures and Materials Performance Laboratory, Institute for Aerospace Research, National Research Council Canada, 1200 Montreal Road, M-3, Ottawa, Ontario K1A 0R6, Canada

JOURNAL OF MECHANICS OF MATERIALS AND STRUCTURES

Journal of Mechanics of Materials and Structures